Kiss, D., Márton, E., Tokarski, A.K. 2016: An integrated paleomagnetic and magnetic anisotropy study of the Oligocene flysch from the Duklanappe, Outer Western Carpathians, Poland. *Geologica Carpathica* 67/6, 595-605.

An integrated paleomagnetic and magnetic anisotropy study of the Oligocene flysch from the Duklanappe, Outer Western Carpathians, Poland

Dániel Kiss[1,2,3], Emő Márton[2], Antek K. Tokarski[4]

[1]Eötvös Loránd University, Department of Geophysics and Space Science, Budapest, Hungary, dan.kiss.91@gmail.com

[2] Geological and Geophysical Institute of Hungary, Paleomagnetic Laboratory, Budapest, Hungary, paleo@mfgi.hu

[3] University of Lausanne, Institute of Earth Sciences, Lausanne, Switzerland

[4] Institute of Geological Sciences, Polish Academy of Sciences, Research Centre in Kraków, Poland, ndtokars@cyf-kr.edu.pl

Keywords

Outer Western Carpathians, Duklanappe, Oligocene flysch, paleomagnetism, anisotropy of magnetic susceptibility, anisotropy of remanence

Abstract

The Dukla Nappe belongs to the Outer Western Carpathians, which suffered considerable shortening due to the convergence and collision of the European and African plates. In this paper we present new paleomagnetic and magnetic anisotropy results from the Polish part

of the Dukla Nappe, based on 102 individually oriented cores from nine geographically distributed localities.

Susceptibility measurements and mineralogy investigations showed that paramagnetic minerals are important contributors of the susceptibility anisotropy (AMS). The AMS fabrics are related to deposition/compression (foliation) and weak tectonic deformation (lineation). The AARM fabric, that of the ferrimagnetic minerals, seems to be less sensitive indicator of tectonic deformation than the AMS fabric.

The inclination-only test points to the pre-folding age of the remanent magnetizations. Seven localities exhibit CCW rotation, a single one shows CW rotation. The CCW rotated paleomagnetic directions form two groups, one showing large, the other moderate CCW rotation. Previously published paleomagentic directions from the Slovakian part of the same nappe exhibit smeared distribution between them. The declination of the overall-mean paleomagnetic direction for the Duklanappe is similar to those observed in the neighbouring Magura and Silesian nappes, but it is of poorer quality.

The AMS lineations at several localities are deviating more to the west from the present north than that of the local tectonic strikes. A possible explanation for this is that the AMS lineations were imprinted first, probably still in the Oligocene, while the sediments were soft (ductile deformation) and the folding and tilting took place during the CCW rotation.

1. Introduction

The Carpathians were formed during the convergence and collision of the European and African plates. Diachronous collision of the two plates started in the Late Jurassic and has continued to the Present. Fragments of continental blocks between the two plates were displaced and rotated in the process of collision and initiated folding/trusting and nappe

transport in the present Outer Carpathians during the Tertiary (Oszczypko, 2006 and references therein). The result is a considerable shortening compared to the original width of sedimentary basins (e.g. Nemčok *et al.* 2000).

The process of the shortening in the Outer Western Carpathians has been investigated with paleomagnetic and magnetic anisotropy methods. Koráb et al., (1981) published paleomagnetic results from the Slovakian part of the Dukla Nappe (Fig. 2) suggesting moderate CCW rotation. They confined their study to localities where the local strike correlated with the general tectonic trend of the nappe. Their results represent red pelitic sediments (Submenilite Beds) of early to middle Eocene age, as the grey sediments sampled by them did not yield stable paleomagnetic signal. Márton et al., (2009) studied the paleomagnetism and the magnetic anisotropy of the Paleogene (subordinately Lower Miocene) grey clay, silt and mudstones from the Magura and the Silesian Nappes. Their results pointed to a general 50°CCW rotation of the Maguranappe and of the central and eastern segment of the Silesian nappe, and somewhat larger for the western part of the Silesian Nappe), which must have taken place after the Oligocene (Márton et al., 2016). The AMS (anisotropy of magnetic susceptibility) measurements revealed that the magnetic foliation was due to compaction and the magnetic lineation to weak compressional deformation. The Czech part of the Outer Western Carpathians was studied extensively with magnetic anisotropy, which revealed that the magnetic fabrics are due to weak tectonic deformation or compaction and sedimentary transport (for a summary see Hrouda et al., 2009).

This study presents new paleomagnetic and magnetic anisotropy results of the Oligocene flysch from the Polish part of the Dukla Nappe. The paleomagnetic directions were obtained

with standard methods, and so were the low field magnetic susceptibility anisotropy (AMS) and the anisotropy of anhystericremanent magnetization (AARM) measurements. Supplementary mineralogy investigations also were carried out to determine the carrier of the remanence and the contributors of the ferri and paramagetnic minerals to the AMS fabric. Finally the data were interpreted in the terms of the rotational and strain history of the nappe.

2. Geological background and sampling

2.1. Geological background

The Carpathians belong to the European Alpine system, which was formed during the convergence and collision of the European and African plates. They have an arcuate shape that extends over 1300km from the Danube valley in Eastern Austria to Danube valley at the border of Romania and Serbia (Fig. 1). The Western Carpathians have been sub-divided into two parts, to the Inner Carpathians and the Outer Carpathians, which are separated by the PieninyKlippen Belt. The Outer Carpathians contain the sediments of several basins that were located between Africa and Stable-Europe during the Cretaceous and Paleogene. The present-day tectonic features were formed mostly in the early-middle Mioceneas a result of the thrusting and folding during the convergence and collision of the ALCAPA and the European plates (Oszczypko, 2006).

The Western Outer Carpathians are a north-verging thrust-and-fold belt composed largely of Lower Cretaceous to Lower Miocene flysch, but Upper Jurassic and Lower Cretaceous volcanics and carbonates are also present (e.g. Kováč&Plašienka, 2002). The studied, Polish part of the belt comprises five rootless nappes that are completely detached from their basement and form an accretionary wedge with northern vergency. The nappes are the

following, from south to north: Magura, Dukla, Silesian, Subsilesian and Skole (Fig. 2.). They are of different lithostratigraphic composition and structure. The wedge is flatly thrust over the Miocene sediments of the Carpathian Foredeep. It is 70-80km wide on the surface and on the south it reaches the depth of 15-20km (Tomek, 1993; Tomek& Hall, 1993). In the traditional view, the wedge started to form in the Oligocene (Pescatore&Ślączka, 1984; Roca et al., 1995; Oszczypko, 2006). More recently synsedimentary deformation studies (Swierczewska&Tokarski, 1998) suggested that deformation in the Magura Nappe started in the Eocene and similar conclusion was reached from balanced cross-sections (Nemčok et al., 2006).

The present study deals with the Polish part of the Dukla Nappe, which continues in Slovakia and in Ukraine and a large part of it is situated below the Magura Nappe (Ślączka et al, 2005). The Magura and Silesian nappes (Fig 2.) are composed of large scale folds and thrust sheets whereas the Dukla and Skolenappes are characterized by imbricated thrusts (e.g. Mastella, 1988).The former nappe shows widespread presence of olistostromes (Cieszkowski et al., 2009). The sequence of the Dukla Nappe starts with Cretaceous sediments and is terminated by the Oligocene Krosno beds. The latter are made of calcareous sandstones and calcareous claystones (Ślączka et al, 2005).

2.2. Paleomagnetic sampling

Based on previous experience with the Outer Western Carpathian Paleogene, the Oligocene Krosno beds were selected for the investigations in the Duklanappe. The mudstone members of the Krosno beds, as documented by the results from the Silesian Nappe (Márton et al., 2009), have favorable lithological properties for palaeomagnetic as well as magnetic anisotropy studies. This formation was sampled at nine geographically distributed localities

(102 individually oriented samples) distributed over the Polish segment of the nappe. At eight localities claystones/mudstones were drilled and at one locality (locality 1) siltstones (1a) and sandstones (1b) were also sampled (Fig 3.). The samples were drilled with a portable drill and oriented *in situ* with a magnetic compass. For each sampled bed, the azimuth and angle of the dip was recorded.

3. Methods

3.1. Paleomagnetic measurements

The samples drilled and oriented in the field were cut into standard-size specimens. The natural remanent magnetization (NRM) of each specimen was measured in the natural state using JR-4 and JR-5A spinner magnetometers. One specimen per sample was stepwise demagnetized with the alternating field (AF) or with thermal method till the NRM signal was lost. It was usually the AF method, which yielded better results. This was due to the carrier of the remanent magnetization, which was magnetite, while the decomposition on heating of the invariably present pyrite resulted in spurious magnetization seriously distorting the NRM signal from 400°C on. The demagnetization curves were analyzed for linear segments and the components decaying towards the origin were evaluated to define the locality mean paleomagnetic directions.

3.2. Anisotropy of magnetic susceptibility (AMS)

AMS provides information about the magnetic fabric. Studying the magnetic fabric has the potential to unravel for example the strain history of the rock and/or sedimentary transport directions. Depending on the value of the mean susceptibility, AMS can be sensitive for

different groups of minerals. If the susceptibility is below or in the range of 10^{-4} [SI] both the ferrimagnetic and the paramagnetic minerals (e.g., pyrite, limonite and Fe bearing clay minerals) can be important contributors to the AMS fabric.

The intensity and orientation of the magnetic fabric is expressed by a second-rank symmetric susceptibility tensor. Geometrically it is represented by an ellipsoid with the $k_{max} \geq k_{int} \geq k_{min}$ principal susceptibilities. In this terminology k_{max} is referring to the magnetic lineation direction and k_{min} is referring to the pole of the magnetic foliation (terms lineation and foliation used in the followings are referring to the magnetic fabric). From the principal directions several parameters can be calculated. In this study we used the following parameters (see Tarling and Hrouda, 1993): degree of anisotropy ($P=k_{max}/k_{min}$), degree of foliation ($F=k_{int}/k_{min}$) degree of lineation ($L=k_{max}/k_{min}$) and mean susceptibility ($k_m=(k_{max}+k_{int}+k_{min})/3$).

The AMS fabric of every individually oriented sample was determined from low field susceptibility measurements in 15 positions with a KLY-2 Kappabridge (Jelínek 1973, 1980). The susceptibility tensor was computed from the results by a program written by Bordás (1990) based on Jelínek (1977). The locality mean tensors were evaluated using the Anisoft 4.2 program (Jelínek, 1978; Hrouda et al., 1990, Chadima and Jelínek, 2008).

3.3. Anisotropy of anhystericremanent magnetization (AARM)

The AARM provides information about the ferromagnetic fabric without the effect of para- and diamagnetic minerals. During the measurement the specimens are firstly demagnetized then magnetized in a given orientation and finally the remanent magnetization is measured. These steps are repeated in several positions and the results are evaluated in a

mathematically analogue way as the susceptibility tensor. The tensor is also represented by an ellipsoid and the same parameters (P, F, L, k_m) are calculated.

During this study, the AARM was measured on specimens, which had not been thermally treated before. The specimens were demagnetized (LDA-3A demagnetizer, at 100mT AF) and magnetized (AMU-1A anhysteric magnetizer, at 80mT AF and 50μT DF) in 12 positions, and the remanent magnetization was measured on JR-4 spinner magnetometer after each magnetization step. The data were computed with AREF program (Jelínek, 1993) and the locality means were evaluated with Anisoft 4.2 (Jelínek, 1978; Hrouda et al., 1990, Chadima and Jelínek, 2008).

3.4. Mineralogy and photo-statistics

During the study magnetic mineralogy experiments, IRM (Isothermal Remanent Magnetization) acquisition and thermal demagnetization of three-component IRM accompanied by the susceptibility monitoring were carried out. These methods are suitable to investigate sediments, they are based on the different coercivites and unblocking temperatures of the magnetic minerals (Lowrie, 1990).

Thin-sections made from some samples were the subjects for a basic petrography. Rock forming minerals were identified and micas and opaque accessories were observed. Polished sections were prepared from a claystone/mudstone and a siltstone sample and ore minerals and their orientation observed. Two samples with similar grain sizes were used for XRD (X-Ray Diffraction) measurements to identify which minerals are present in larger concentration than 5%.

Oriented thin-sections cut along the bedding plane were used for photo statistics to unravel the statistical alignment of elongated particles. This method has been used previously to

determine sedimentary transport direction in ignimbrites (Capaccioniand Sarocchi 1996, Capaccioni et al., 1997, Biró et al., 2015). The x and z directions were marked on the thin sections, so the comparison between the anisotropy principal directions and any grain fabric orientation direction was possible. For the photo-statistical grain shape analysis the scanned thin-sections (scanned with 2000 dpi resolution) were processed in ENVI EX 4.8 and ESRI ArcGIS 10.0 Desktop environment. ENVI EX 4.8 was used for automatized detection of grains based on spatial and spectral features. On the scanned images individual minerals (especially mica) are not distinguishable so microphotos were also made. As the contrast was too small for the automatized method, distinguishable micas were digitized manually. The azimuth of the a-axis and the elongation (a-axis/b-axis) of each grain-derived polygon were calculated using the Zonal Geometry as Table Tool function of ESRI ArcGIS 10.0. Further processing of the attributes related to individual grains was made using GEOrient 9.5 software.

4. Results

4.1. Paleomagnetism

The paleomagnetic directions with statistical parameters were determined for eight localities (Table 1). The locality mean paleomagnetic directions are highly scattered before tilt corrections (Fig. 4a). After correction for local tilts, the inclinations become less scattered than before, the inclination-only test is positive at 100% for the seven CCW rotated localities (k_2/k_1=3.95 with the limit=2.69 and I°=+49.7°) and for all of the localities (k_2/k_1=3.48 with the limit=2.48 and I°=+47.4°), suggesting that the remanences were acquired before folding. The above inclinations are shallower than the expected inclinations in a European framework (+59.7° and +63.4° calculated from the European APWs by Besse and Courtillot 2002 and Torsvik et al. 2012, respectively). Five locality mean directions cluster (localities 1a, 4, 7, 8

and 9), exhibiting large CCW rotations. Two of the remaining localities (3 and 5) suggest significantly smaller CCW rotation, one locality (6) exhibits CW rotated declination (Fig. 4b).

4.2. Anisotropy of Magnetic Susceptibility (AMS)

AMS measurements revealed that the locality mean susceptibilities are in a range of $1\text{-}3*10^{-4}$ [SI] and the degrees of anisotropy are between 0.9% and 8.7% (Table 2). For most localities, the AMS fabrics are foliated and the minimum directions are sub-vertical after tilt correction. Exceptions are localities 1, 6 and some samples from locality 2. The AMS fabrics of both the siltstone (1a) and the sandstone (1b) are lineated and the poles of foliations are somewhat deflected from the vertical. Samples from locality 6, and three samples from locality 2 (drilled from the same bed) exhibit horizontal poles of foliations (Fig. 5), and the magnetic fabric is inverse (PL 1456, 0°C; max: 336/72, int: 74/3, min: 165/18). Inverse fabric can be due to the presence of either single domain magnetite or siderite (Tarling and Hrouda 1993, Chadima et al., 2006). In the present case, after heating the samples to 460°C, the fabric becomes normal (PL 1456, 460 °C max: 162/18, int: 71/5, min: 327/71), which points to the decomposition of siderite, similarly to the case in the Skolenappe, (Márton et al., 2010).

All localities, no matter if the fabrics are dominantly foliated or lineated, are characterized by well-defined AMS lineations. Some of them are aligned with the general NW-SE tectonic trend of the Duklanappe, others are quite different (Fig.3).

4.3. Anisotropy of AnhystericRemanent Magnetization (AARM)

The sandstone at locality 1 (1b) exhibits highly scattered AARM directions, and only two samples were measurable from locality 2. For the rest, the AARM fabrics are dominantly foliated (Table 2). As in the case of AMS, the foliation poles are typically within 10° of the

vertical, except at localities 1a and 9. AARM lineations are well grouped on locality level for localities 4, 5, 6, and 7, but exhibit moderate or large scatter at the other localities.

4.4. Mineralogy and photo-statistics

The IRM acquisition curve and the three-component IRM demagnetization show that a low-coercivity mineral dominates. It is most probably magnetite, since the IRM signal is still existing at the temperature of dramatic increase of the susceptibility at 400°C (probably due to decomposition of pyrite) which prevents obtaining stable IRM components up to the Curie point of magnetite. The simultaneous existence of magnetite and pyrite in the Krosno beds was also observed in the Silesian Nappe (Márton et al., 2009).

In thin sections quartz and carbonates as main ingredients but also opaque minerals, limonite and mica (mostly in the siltstone) were found. Ore-microscopy proved that the opaque minerals are indeed magnetite and pyrite (Fig. 7.). The XRD measurements showed that in addition to quartz, calcite, dolomite, albite more than 5 percent of clay minerals, probably with Fe content, are present in the studied samples.

The 2000 dpi resolution was not enough to detect the required number of grains in the claystone/mudstone thin-sections and also they lacked the required number of micas for statistical evaluation. In the siltstone both methods (scanned image and micro photo) revealed a lineated fabric, but the directions obtained are perpendicular to each other (Fig. 8.).

5. Discussion

The majority of, the Oligocene paleomagnetic directions from the Polish part of the Duklanappe indicate CCW rotation. In this sense, the situation is similar to the Slovakian part

of the nappe (Koráb et al., 1981) and to the Silesian and the Maguranappes (Márton et al., 2009). However, in the Polish part of the Duklanappe the locality mean paleomagnetic directions define three groups, the majority of the localities exhibit large, two localities moderate CCW rotations (Fig. 4.b.) and one locality (6) suggests CW rotation.

It was mentioned in a previous section that some of the locality mean paleomagentic inclinations, after tilt correction, are shallower, than those expected in a European framework. Therefore, we investigated the possibility of inclination flattening, which is a well-known phenomenon in clastic sediments, and it is related to compaction. The degree of the anisotropy of remanence, which is the expression of the fabric of the ferromagnetic minerals, can be used to decide if the paleomagnetic inclination could have been flattened. According to Stephenson et al., (1986) inclination flattening can be ruled out if the degree of AARM anisotropy (P) is lower than 5 percent. The P parameters we measured exceed this limit (Table 2). However, they are very similar (7.3-11.7%) for localities with higher and lower inclinations (Table 1), and there is only a weak correlation (R^2=0.19) between the locality mean inclinations and the degree of AARM anisotropy. Thus, it is more likely that a small, unremovable overprint is responsible for shallower than expected inclinations or the magnetization was acquired during folding, as the cluster of the locality mean paleomagneitc directions is tightest at 45% unfolding.

The Slovakian part of the Duklanappealso suggests a general CCW rotation (Koráb et al., 1981). Disregarding locality 6, which is an outlier, the overall-mean paleomagentic direction for the Polish segment of the nappe is D°=312.3°, I°=+57.3°, k=9.2, □□20.9°, N=7 (synfolding at 45% unfolding). This result, combined with the tilt corrected locality mean directions for the Slovakian segment (Koráb et al., 1981, neither directions before tilt corrections not the tectonic tilt is documented), yields D°=328.0°, I°=+50.7°, k=9.7, □□14.7°, N=12. The general

CCW rotation is poorly constrained in both cases. Nevertheless, they are in line with the findings from the neighboring Silesian and Maguranappes (Márton et al., 2009, Fig. 9).

Tectonic deformation in the Duklanappe produced imbricated thrusts in the large scale and also imprinted the dominantly sedimentary magnetic fabrics. The deformation must have been weak, since pencil fabric occurs only at a single locality (Fig. 5). Well-defined AMS lineations (on locality level) are typical, which are related to tectonic deformation as the principal agent for the following reasons. One is that the studied samples (except locality 1b) are fine-grained, and they were deposited in the final stage of sedimentiation from a turbidite. Furthermore, the samples typically represent more than one bed from the same locality, yet the AMS lineation directions are well grouped on locality level. Finally, the AMS lineations correlate with the local strikes. However, the local strikes and the corresponding AMS lineations are variable within the Duklanappe. Some are near-parallel to the general trend of the nappe, some are close to N-S or E-W. Assuming that this phenomenon is due to local tectonic disturbances, we can apply “rotation corrections” for the palaeomagneticdeclinations. The method uses the angle and sense of deviation from the general NW-SE tectonic trend of the nappe as correcting factor. The correction resulted in more incoherent paleomagnetic directions than before. When AMS lineations are used as proxies for the strikes the result is similar. Thus, local tectonic disturbances in the form of local rotations are not likely to explain the deviations from the general trend of the nappe. A more likely mechanism may be the strain partitioning within the nappe.

The studied localities typically exhibit AMS lineations, which systematically depart in the CCW sense from the respective local strikes (Fig.10). This phenomenon suggests that the ductile deformation resulting in the AMS lineationscommenced before the folds were

formed, i.e. the former came into being while the sediments were soft, probably still in the late Oligocene, the latter somewhat later, during the rotation process.

The fabrics of the magnetic minerals (AARM) seem to be less sensitive to deformation than those of the AMS. In the sandstone of locality 1 (1b) is not oriented (solemarks show that strong paleocurrents affected the sandstone beds). At the other localities the AARM foliation similarly to the AMS foliation near-parallel to the bedding plane. AARM lineations are quite scattered in the siltsone of locality 1 and localities 3 and 9 and the mean AARM lineation directions are different from those of the AMS lineations. We infer that the ferromagnetic grains in these cases were basically oriented by sedimentary transport, since in the siltstone of locality 1 the micas seem perpendicularly arranged with respect to the iron minerals (Fig. 8.), i.e. they are imbricated by the current.

At the remaining localities, the AARM lineations are clustered on the locality level. At localities 4, 7, 8 and 6 (at the last after the decomposition of siderite), the AMS and AARM lineations are close to each other. Thus, at these localities the AARM lineations may be of the same origin as the AMS lineations. At locality 5 the AARM lineation is very well defined, yet it is almost perpendicular to the AMS lineation. In this case, the ferrimagentic grains must have been quite strongly oriented by water flow, and could not be affected by weak compression.

6. Conclusions

The susceptibility measurements indicated and mineralogy investigations (magnetic mineralogy, petrography, ore-microscopy and XRD) confirmed that paramagnetic minerals are important contributors to the AMS fabric of the Krosno beds of the Duklanappe. The contribution of the ferromagnetic mineral to the AMS (identified by IRM experiment and

ore-microscopy as magnetite), must be subordinate, since it is present in very low concentration.

At most localities, the AMS foliation is practically bedding parallel, indicating that the deformation was weak. Early stage pencil structure was observed only at one locality, suggesting somewhat stronger deformation.

AMS lineation directions, which are fairly well defined, can be related to local tectonic strikes, so they are due to tectonic deformation. However, there are several cases where neither the local strike, nor the AMS lineation correlates with the general strike of the Duklanappe. It is quite likely that strain partitioning is responsible for the observed distribution of the markers of extension directions.

In some cases AMS and AARM ellipsoids (the latter reflects the orientation of the ferromagnetic grains) are not coaxial and the AARM lineations are quite scattered. Thus, we can conclude that the paramagnetic fabric is more sensitive to deformation than the ferrimagnetic fabric, which preserves the characteristics of a flow-oriented arrangement of the magnetic grains.

The palaeomagneticlocality mean inclinations respond positively to the inclination-only test. However, the declinations define three groups. One with five members exhibits large, the second with two members small CCW rotations, while the third has only one locality indicating slight CW rotation. “Rotation corrections” were applied to remove the effect of possible local rotations, but they resulted in a more scattered picture. Thus, local tectonic rotation postdating the acquisition of the remanence cannot account for the results.

It is beyond doubt that the Dukla Nappe suffered post-Oligocene CCW rotation, but the magnitude is statistically poorly defined. The orientations of the AMS lineations at several localities are deviating more to the west from the present north than that of the

local tectonic strikes. A possible explanation for this is that the AMS lineations were imprinted first, probably still in the Oligocene, while the sediments were soft (ductile deformation) and the folding and tilting took place during the CCW rotation.

Acknowledgements

We thank Tamás Biró, István Dódony, Gabriella Kiss and Sándor Józsa for their guidance to carry out the non-magnetic mineralogy investigations and we also thank the Eötvös Loránd University for providing access to the instruments and the laboratories. We thank Ludivine Sadeski, a student of EOST - University of Strasbourg, who started the AARM measurements of the samples from the Dukla during her internship at the Paleomagnetic Laboratory. This work was partly financed by the Hungarian Research Fund (OTKA) project no. K105245 and from a joint project of the Academies of Science of Poland and Hungary.

References

Besse J. & Courtillot V. 2002: Apparent and true polar wander and the geometry of the geomagnetic field over the last 200 Myr. *Journal of Geophysical Research,* 107, 6, 1-31.

Biró T., Karátson D., Márton E., Józsa S. & Bradák B. 2015*:* Paleoflow directions from a subaqueous lahar deposit around the Miocene Keserűs Hill lava dome complex (north Hungary) as constrained by photo-statistics and anisotropy of magnetic susceptibility (AMS). *Journal of Volcanology and Geothermal Research,* 302, 141-149.

Bordás, R. 1990: Aniso – Anisotropy program package for IBM PC. ELGI, Budapest.

Capaccioni B. & Sarocchi D. 1996: Computer-assisted image analysis on clast shape fabric from the Orvieto-Bagnoregio ignimbrite (Vulsini District, central Italy): implications on the emplacement mechanisms. *Journal of Volcanology and Geothermal Research*, 70, 1-2, 75-90.

Capaccioni B., Valentini L., Rocchi M.B.L., Nappi G. & Sarocchi D. 1997: Image analysis and circular statistics for shape-fabric analysis: applications to lithified ignimbrite. *Bulletin of Volcanology*, 58, 7, 501-514.

Chadima M., Pruner P. & Sletcha S. 2006: Magnetic fabric variations in Mesozoic black shales, northern Siberia, Russia: Possible paleomagnetic implications. *Tectonophysics*, 418, 1-2, 145-162.

Chadima M. & Jelínek V. 2008: Anisoft 4.2. – Anisotropy data browser. Contrib. Geoph. Geod., 38, 41.

Cieszowski M., Golonka J., Krobicki M., Ślączka A, Oszczypko N., Waśkowska A. & Wendorff M. 2009: The Northern Carpathians plate tectonic evolutionary stages and origin in of olistoliths and olistostromes. *GeodinamicaActa*, 22, 1-3, 1-26.

Fisher R. 1953: Dispersion on a sphere. *Proc. Roy. Soc. Lond. Ser. A.,* 217,295–305.

Hrouda F., Jelínek V. & Hrušková L. 1990: A package of programs for statistical evaluation of magnetic anisotropy data using IBMPC computers. *EOS Trans. AGU*. Fall meeting 1990.

Hrouda F., Krejčí O., Potfaj M. & Stráník Z. 2009: Magnetic fabric and weak deformation in sandstones of accretionary prisms of the Flysch and Klippen Belts of the Western Carpathians: Mostly offscraping indicated. *Tectonophysics*, 479, 254-270.

Jelínek V. 1973: Precision A. C. bridge set for measuring magnetic susceptibility of rocks and its anisotropy. *Studiageophys. geod.*, 17, 1, 36–48.

Jelínek V. 1977: The statistical theory of measuring anistropy of magnetic susceptibility of rocks and its application. *Geofyzika*, s.p., Brno.

Jelínek V. 1978: Statistical processing of magnetic susceptibility measured on groups of specimens. *Studiageophys. geod.,* 22, 1, 50–62.

Jelínek V. 1980: Kappabridge KLY-2. A precision laboratory bridge for measuring magnetic susceptibility of rocks (including anisotropy).Leaflet, *Geofyzika,* Brno.

Jelínek V. 1993: Theory and measurement of the anisotropy of isothermal remanent magnetization of rocks. *Trav. Geophys.,* 37, 124–134.

Kirschvink J.L. 1980: The least-squares line and plane and the analysis of palaeomagnetic data. *Geophys. J.R. astr. Soc.,* 62,699–718.

Koráb T., Krs M., Krsová M. & Pagáč P. 1981: Paleomagnetic Investigations of Albian(?) – Paleocene to Lower Eocene Sediments from the Dukla Unit, East Slovakian Flysch, Czechoslovakia. ZápadnéKarpaty, sérgeológia 7. *Geol. Úst. D. Štúra*, Bratislava, 127-149.

Kováč M. & Plašienka D. 2002: Geological Structure of the Alpine-Carpathian-Pannonian Junction and Neighbouring Slopes of the Bohemian Massif. University textbook. *Comenius University*, Bratislava, 17-24.

Krs M., Krsová M., Chvojka R. & Potfaj M. 1991: Paleomagnetic investigations of the flysch belt in the Orava region, Magura unit, Czechoslovak Western Carpathians. Geologickeprace, DionýzStúr Geological Institute, Bratislava, 92, 135-151.

Lowrie W. 1990: Identification of ferromagnetic minerals in a rock by coercivity and unblocking temperature properties. *Geophys. Res. Lett*., 17, 2,159–162.

Márton E., Rauch-Włodarska M., Krejčí O., Tokarski A.K. & Bubík M. 2009: An integrated palaeomagnetic and AMS study of the tertiary flysch from the Outer Western Carpathians. *Geophys. J. Int.*, 177, 3, 925−940.

Márton E., Bradák B., Rauch-Włodarska M. & Tokarski A.K. 2010: Magnetic anisotropy of clayey and silty members of tertiary flysch from the Silesian and SkoleNappes (Outer Carpathians). *Stud. Geophys. Geod.*, 54, 121−134.

Márton E., Grabowski J., Tokarski A.K. & Túnyi I. 2016: Palaeomagnetic results from the fold and thrust belt of the Western Carpathians: an overview. In: Pueyo E. L., Cifelli F., Sussman A. J. &Oliva-Urcia, B. (eds) Palaeomagnetism in Fold and Thrust Belts: New Perspectives. Geological Society, London, Special Publications, 425, 7-36.

Mastella L. 1988: Structure and evolution of MszanaDolna tectonic window, Outer Carpathians, Poland. *AnnalesSocietatisGeologorumPoloniae*, 58, 1-2, 53-173 (in Polish with English summary).

Mattei M., Sagotti L., Faccena C., Funiciello R. 1997: Magnetic fabric of weakly deformed clay-rich sediments in the Italian peninsula.: Relationship with compressional and extensional tectonics. *Tectonophysics*, 271, 107-122.

Nemčok M., Krzywiec P., Wojtaszek M., Ludhová L., Klecker R.A., Secombe W.J. & Coward M.P. 2006: Tertiary development of the Polish and eastern Slovak parts of the Carpathian accretionary wedge: insights from balanced cross-sections. *Geol. Carpathica,* 57, 5, 355–370.

Nemčok M., Nemčok J., Wojtaszek M., Ludhova L., Klecker R.A., Sercombe W.J., Coward M.P. & Keith J.F. Jr. 2000: Results of 2D balancing along 20° and 21°30’ longitude and pseudo-3D in the Smilno tectonic window: Implications for shortening mechanisms of the West Carpathian accretionary wedge. *Geol. Carpathica,* 51, 5, 281–300.

Oszczypko N. 2006: Late Jurassic-Miocene evolution of the Outer Carpathian fold-and-thrust belt and its foredeep basin (Western Carpathians, Poland), *Geol. Quat.,* 50, 1, 169–194.

Pescatore T. & Ślączka A. 1984: Evolution models of two flysch basins: the Northern Carpathians and Southern Appennines. *Tectonophysics,* 106, 1-2, 49–70.

Roca E., Bessereau G., Jawor E., Kotarba M. & Roure F. 1995: Pre-Neogene evolution of the Western Carpathians: Constructions from the Bochnia-TatraMoutains section (Polish Western Carpathians). *Tectonics,* 14, 4, 855–873.

Stephenson A., Sadikun S. & Potter D.K. 1986: A theoretical comparison of the anisotropies of magnetic susceptibility and remanence in rocks and minerals. *Geophysical Journal of Royal Astronomical Society,* 84, 185-200.

Ślączka A., Krugłov S., Golonka J., Oszczypko N. &Popadyuk I. 2005: Geology and Hydrocarbon Resources of the Outer Carpathians, Poland, Slovakia, and Ukraine: General Geology. In: J. Golonka and F. J. Picha (Eds.): The Carpathians and their foreland: Geology and hydrocarbon resources: AAPG Memoir 84. *AAPG*, 221 – 258.

Świerczewska, A. & Tokarski, A.K., 1998: Deformation bands and the history of folding in the MaguraNappe,Western Outer Carpathians (Poland). *Tectonophysics,* 297,1-4,73–90.

Tarling D.H. &Hrouda F. 1993: The Magnetic anisotropy of rocks. *Chapman & Hall,* London.

Tomek Č. & Hall J. 1993: Subducted continental margin imaged in the Carpathians of Czechoslovakia. *Geology,* 21, 6, 535–538.

Tomek, Č. 1993: Deep crustal structure beneath the central and inner West Carpathians, *Tectonophysics*.226, 1-4, 417-431.

Torsvik T. H., Müller D. M., Van der Voo R., Steinberger B. & Gaina C. 2008: Global Plate Motion Frames: Toward a Unified Model, Reviews of Geophysics, 46, RG3004, 1-44.

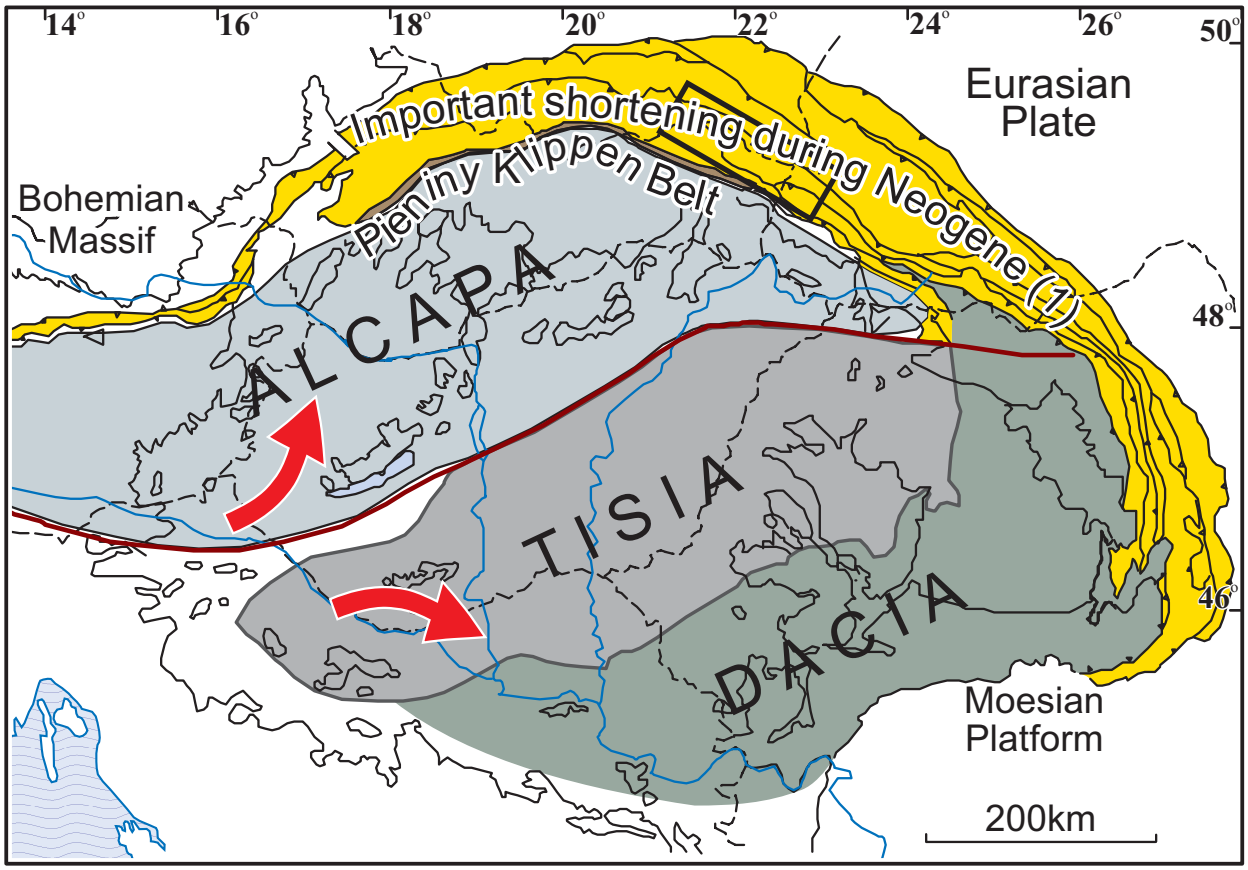

Fig. 1. The tectonic subdivision of the Carpatho–Pannonian region. The yellow area of the Outer Carpathians characterized by Tertiary nappe transport and the arrows refer to the rotation of the microplates (after Márton et al., 2009). The study area is indicated (for more precise location see Fig. 2. and 3.)

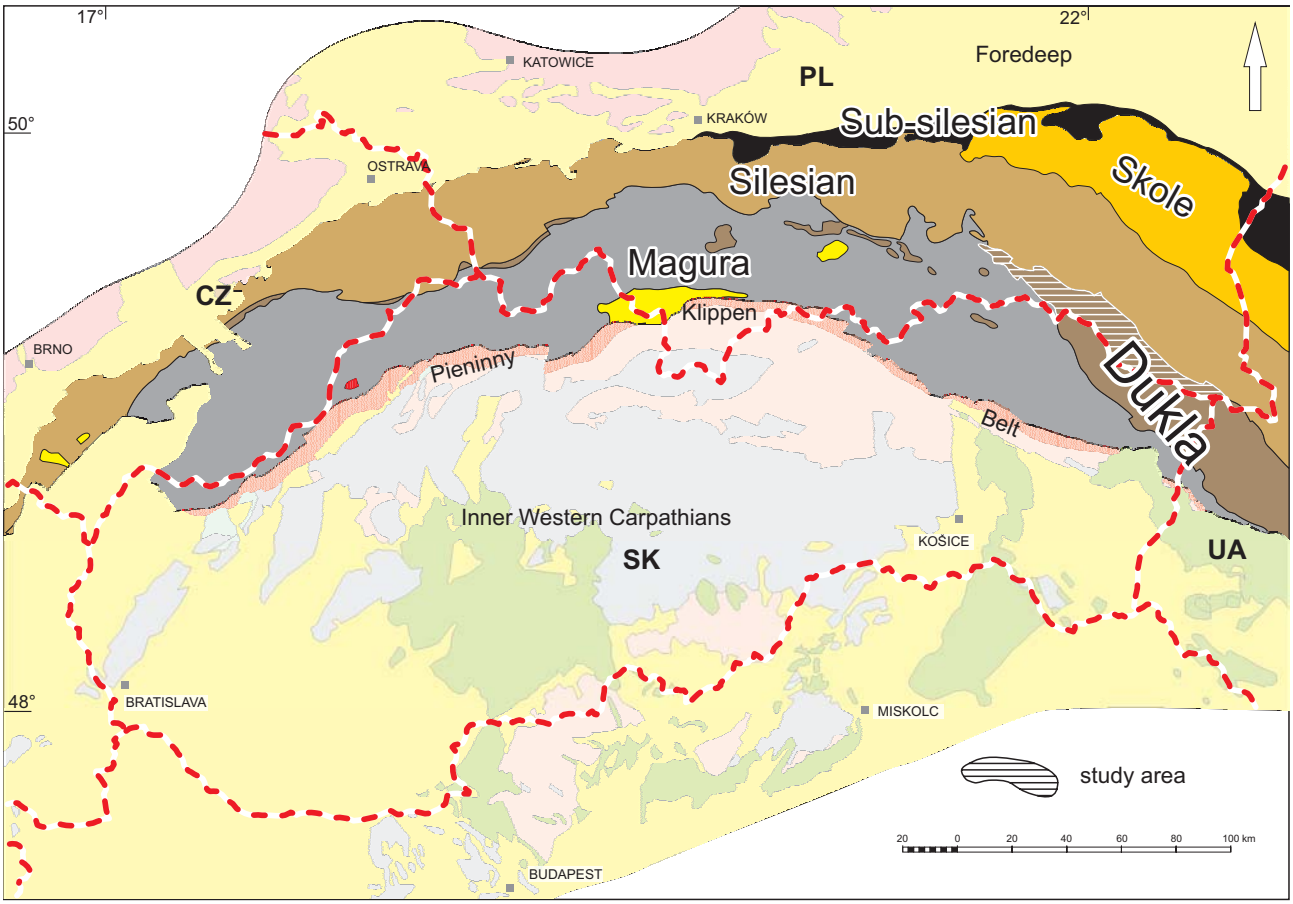

Fig. 2. The location and structure of the Outer Western Carpathians (dark) (the SubsilesianNappe - located at the northern boundary of the Silesian nappe - is not indicated).

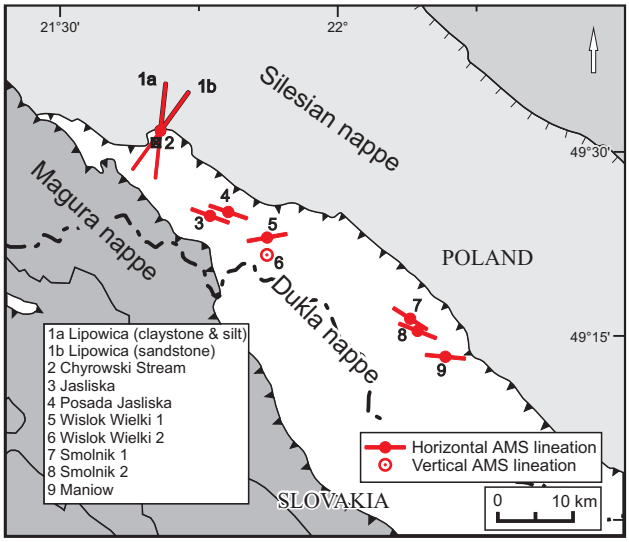

Fig. 3. The Polish part of the DuklaNappe, with the localities and the locality mean AMS lineation directions (at locality 1 directions are enlarged for better visibility and at locality 2 locality mean direction cannot be given).

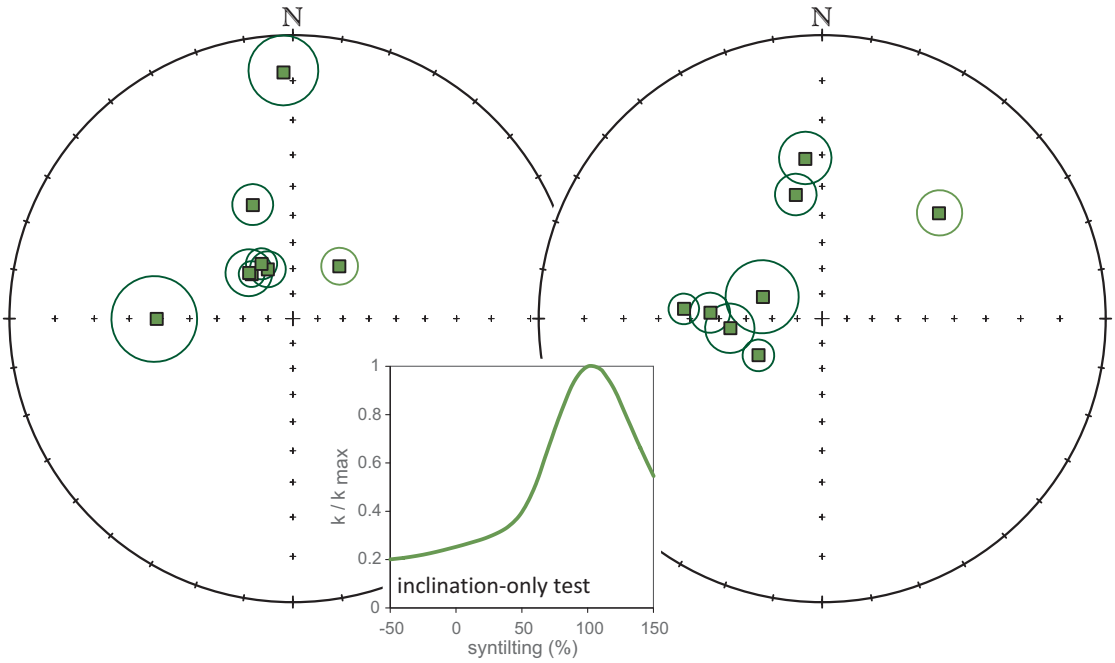

Fig. 4. Locality mean paleomagnetic directions with a_{95} before (left side) and after (right side) tilt correction shown in lower hemisphere equal angle projections and the inclination-only test.

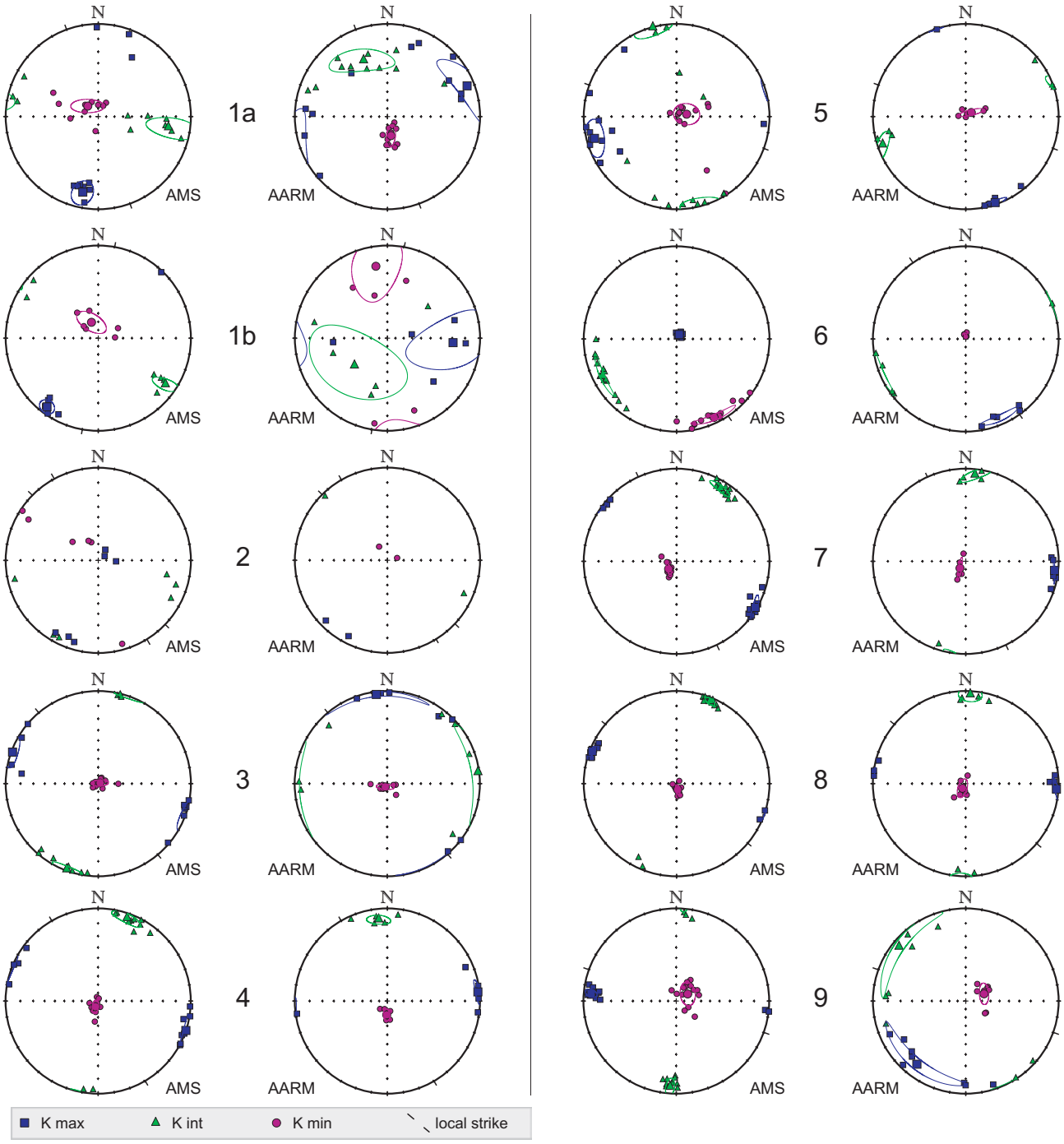

Fig. 5. Anisotropy directions of the studied localities on lower hemisphere equal angle projections. In the most case foliation is dominant (exceptions: AMS 1a, AMS 1b, AMS 6).

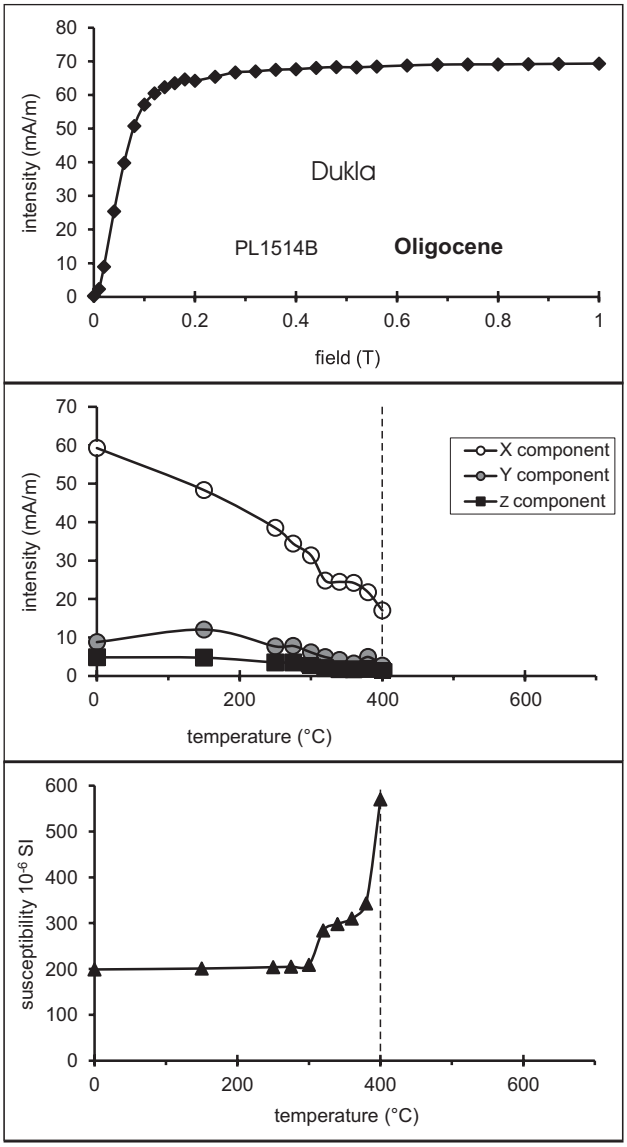

Fig. 6. IRM acquisition, normalized three- component IRM demagnetization and susceptibility vs. temperature curves (from top to bottom). The IRM saturates fast (0.2T) which refers to low-coercivity magnetic minerals and the three-component IRM demagnetization also supports that. There is an increase of susceptibility after 300°C, which is typical for iron-sulphides. After 400°C (vertical, dashed line) the susceptibility is increasing dramatically which shows that the sample became unstable, so the demagnetization have not been continued.

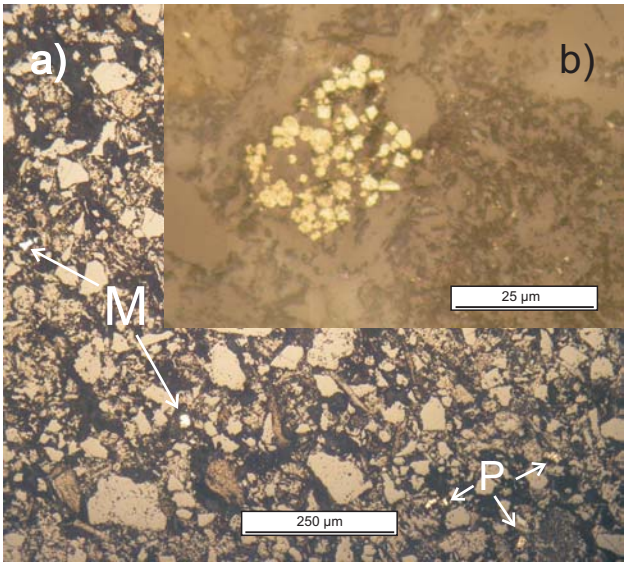

Fig. 7. Ore-microscopy images of polished thin sections. Pyrite (P) and magnetite (M) were recognized as ore-minerals (Fig. a). The pyrite is characterized by framboidal structure (Fig. b).

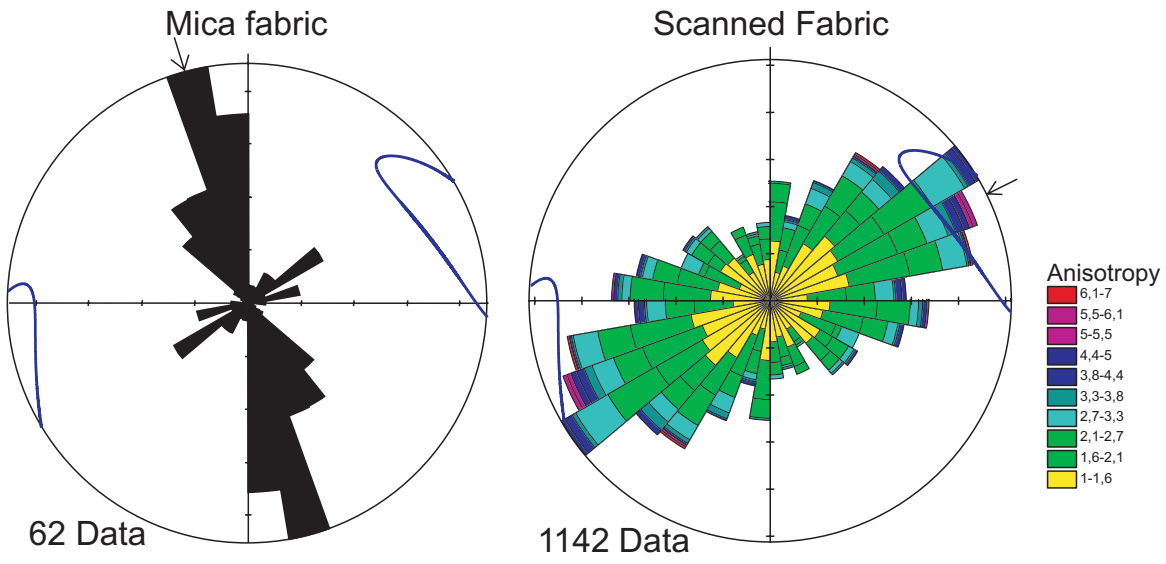

Fig. 8. The distribution of particle long-axis orientations in the plane of bedding (after tilt correction). The data was obtained by photo-statistics from a siltstone pilot sample (PI 1521) from locality 1a. Both the scanned particles (a) and the micas (b) show lineation, but they are perpendicular to each other. Most probably the micas are imbricated by the paleoflow so they are apparently lineated perpendicular to the flow direction in the bedding parallel section. The elongated scanned particles are aligned parallel to the paleoflow, therefore both methods refers to the same sedimentary transport direction, which lies within the confidence interval of the AARM lineation of locality 1a.

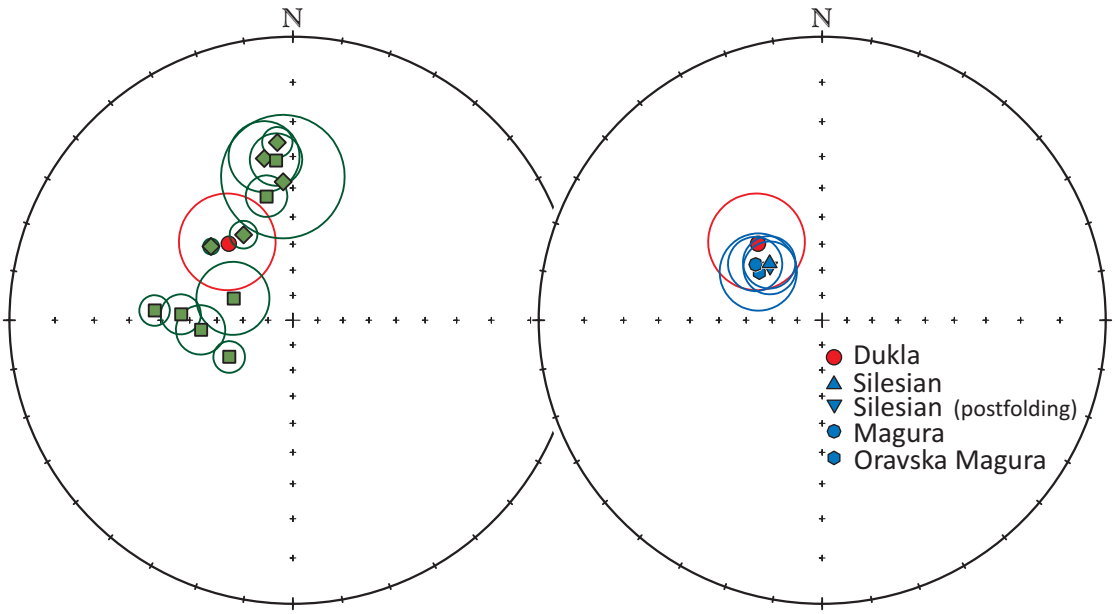

Fig. 9. Locality meanpaleomagnetic directions with a_{95} from both the Polish (this study, without the outlier locality 6) and the Slovakian (Koráb et al., 1981) parts of the nappe (squares and diamonds, respectively), and the overall mean direction of the nappe (full circle) with a_{95} (left side). The overall mean paleomagnetic directions of Dukla Nappe, Magura Nappe, Oravska Magura (Krs et al., 1991), Silesian Nappe (Central + Eastern part, prefolding magnetization, Márton et al., 2016) and Silesian Nappe (Eastern part postfolding magnetization, Márton et al., 2009) (right side).

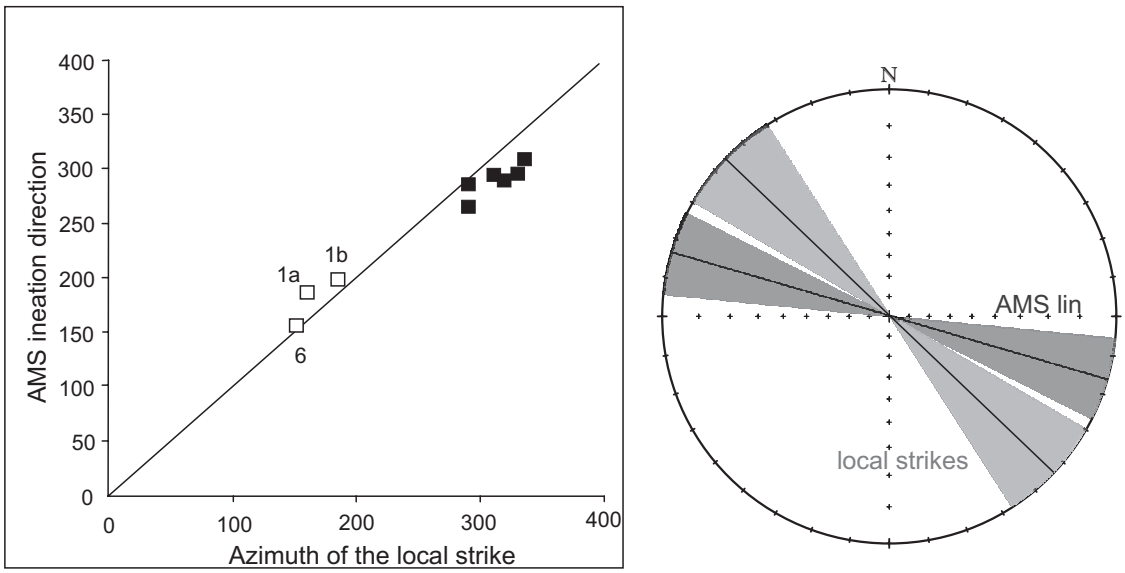

Fig. 10. On the left the AMS directions are plotted as a function of the local strike, and the 45° line is indicated. All points are close to the reference line, the AMS lineation directions correlate with the local strikes at all localities, but the points are located systematically below the line except three points. Localities 1a and 1b are above the line and locality 6 is on the line (here the AARM lineation is indicated due to the presence of siderite). The mean AMS lineation and strike directions with confidence intervals of the six localities are shown on the right. This systematical westward deflection of the AMS lineations coincides with the general CCW rotation.

	Locality	Lat.N, Lon.E	Lithology	n/no	D°	I°	K	α_{95}°	D_C°	I_C°	k	α_{95}°	dip
1a	Lipowica 1 PL 1514-527	49°31'43" 21°40'51"	claystone silt	12/14	90	-39	11	14	110	-65	11	14	70/30
1b	Lipowica 2 PL 1555-561	49°31'49" 21°40'45"	sandstone	0/7	Unstable NRM								280/40 280/60
2	Lipowica stream PL 1562-567	49°31'30" 21°41'04"		0/6	Disintegrated during measurement								45/45 60/30
3	Jaśliska PL 1258-269	49°26'09" 21°48'07"		11/12	341	+44	43	7	348	+42	43	7	50/8
4	PosadaJaślisk a PL 1445-455	49°26'34" 21°28'17"		10/11	334	+68	51	7	273	+47	51	7	240/40
5	Wisłok Wielki PL 1246-257	49°24'27" 21°58'49"	claystone/ mudstone	12/12	178	-8	32	8	174	-31	32	8	200/25
6	Wisłok Wielki 2 PL 1456-467	49°23'19" 21°59'28"		11/12	42	+62	42	7	48	+32	42	7	55/30
7	Smolnik 1 PL 1409-420	49°15'21" 22°06'56"		8/12	318	+66	115	5	274	+38	115	5	245/40
8	Smolnik 2 PL 1421-432	49°14'38" 22°07'58"		10/12	317	+65	32	9	264	+54	32	9	220/30
9	Michów PL 1395-408	49°13'18" 22°11'38"		13/14	331	+65	44	6	240	+61	44	6	200/40

Table 1. Summary of locality mean palaeomagnetic directions based on the results of principal component analysis (Kirschvink 1980). Localities are numbered according to Fig. 3.

Key: Lat.N, Lon.E: Geographic coordinates (WGS84) measured by GPS, n/no: number of used/collected samples (the samples are independently oriented cores); D, I (Dc, Ic): declination, inclination before (after) tilt correction; k and α_{95}: statistical parameters (Fisher, 1953).

	Locality		N	mean K (10^{-6}SI)	Max. D°	Max. I°	conf. angle	Int. D°	Int. I°	conf. angle	Min. D°	Min. I°	conf. angle	P(%)	L(%)	F(%)
1a	Lipowica, clay and silt PL 1514-527	AMS	12	155	192	9	8/7	99	18	20/18	307	70	20/8	0,9	0,6	0,3
		AARM	10		67	4	26/7	336	21	27/9	167	68	13/6	8,2	2,5	5,6
1b	Lipowica, sandstone PL 1555-561	AMS	6	69	217	8	8/5	125	13	15/4	336	75	15/7	1,4	0,9	0,6
		AARM	6		significant scatter											
2	Lipowica stream PL 1562-567	AMS	6		two AMS clusters of 3-3 samples, statistics cannot calculated for less than 5 samples											
		AARM	2													
3	Jasliska PL 1258-269	AMS	12	222	290	2	10/7	200	1	10/4	76	88	7/3	6.7	0.8	5.8
		AARM	8		353	3	35/3	83	2	35/8	220	86	8/2	7.3	0.9	6.3
4	Posade Jasliska PL 1421-432	AMS	11	186	109	1	11/3	19	6	11/5	210	84	6/3	7.8	0.6	7.1
		AARM	5		84	2	8/3	354	12	9/5	184	78	5/3	11.7	1.9	9,6
5	Wislok Wielki 1 PL 1246-257	AMS	13	210	255	9	14/11	345	0	13/10	76	81	12/9	0.8	0.3	0.6
		AARM	6		161	2	8/3	251	6	13/5	53	84	11/2	10.2	1.4	8.6
6	Wislok Wielki 2 PL 1456-467	AMS	8	287	35	81	3/1	240	8	18/1	150	4	18/1	4.8	4.2	0.5
		AARM	5		156	4	14/2	247	1	14/2	352	86	2/2	11.3	2.3	8.8
7	Smolnik 1 PL 1409-420	AMS	12	235	121	3	9/3	30	10	9/3	229	80	5/2	8.7	0.6	8.1
		AARM	5		96	5	9/1	5	6	13/4	226	82	10/2	10.3	2.3	7.8
8	Smolnik 2 PL 1421-432	AMS	6	195	291	2	4/2	22	5	5/1	175	85	3/2	7.8	1.4	6.3
		AARM	6		102	4	22/5	12	4	22/8	238	85	8/6	9,4	2.1	7.1
9	Maniow PL 1395-408	AMS	14	166	275	9	7/3	184	7	10/3	58	78	10/7	3.1	1.0	2.1
		AARM	7		225	16	30/6	317	7	30/7	69	73	10/4	8.3	1.0	7.3

Table 2. Summary of tilt corrected locality mean anisotropy directions (both AMS and AARM). Localities are numbered according to Fig. 3 and lithology is claystone/mudstone except if it is stated otherwise.